Error-free transmission of microring-modulated BPSK

Kishore Padmaraju,[1,*] Noam Ophir,[2] Qianfan Xu,[2] Bradley Schmidt,[2] Jagat Shakya,[2] Sasikanth Manipatruni,[2] Michal Lipson,[2,3] and Keren Bergman[1]

[1]*Department of Electrical Engineering, Columbia University, 500 West 120th Street, New York, New York, USA*
[2]*School of Electrical and Computer Engineering, Cornell University, 428 Phillips Hall, Ithaca, New York, USA*
[3]*Kavli Institute at Cornell, Ithaca, New York, USA*
**kpadmara@ee.columbia.edu*

Abstract: We demonstrate the generation of error-free binary-phase-shift-keyed (BPSK) data at 5 Gb/s using a silicon microring modulator. The microring-modulated BPSK signal is propagated at fiber lengths up to 80 km, maintaining error-free performance, while demonstrating resilience to chromatic dispersion. Bit-error-rate measurements and eye diagrams show near equivalent performance of a microring-based BPSK modulator as compared to commercial $LiNbO_3$ phase modulators.

OCIS codes: (060.5060) Phase modulation; (230.3120) Integrated optics devices.

References and links

1. P. E. Green, "Fiber to the home: the next big broadband thing," IEEE Commun. Mag. **42**(9), 100–106 (2004).
2. D. P. Shea and J. E. Mitchell, "Long-reach optical access technologies," IEEE Netw. **21**(5), 5–11 (2007).
3. B. E. Little, J. S. Foresi, G. Steinmeyer, E. R. Thoen, S. T. Chu, H. A. Haus, E. P. Ippen, L. C. Kimerling, and W. Greene, "Ultra-compact Si/SiO_2 microring resonator optical channel dropping filters," IEEE Photon. Technol. Lett. **10**(4), 549–551 (1998).
4. A. Liu, R. Jones, L. Liao, D. Samara-Rubio, D. Rubin, O. Cohen, R. Nicolaescu, and M. Paniccia, "A high-speed silicon optical modulator based on a metal-oxide-semiconductor capacitor," Nature **427**(6975), 615–618 (2004).
5. Q. Xu, B. Schmidt, S. Pradhan, and M. Lipson, "Micrometre-scale silicon electro-optic modulator," Nature **435**(7040), 325–327 (2005).
6. H. L. R. Lira, S. Manipatruni, and M. Lipson, "Broadband hitless silicon electro-optic switch for on-chip optical networks," Opt. Express **17**(25), 22271–22280 (2009).
7. J. Van Campenhout, W. M. J. Green, S. Assefa, and Y. A. Vlasov, "Low-power, 2 x 2 silicon electro-optic switch with 110-nm bandwidth for broadband reconfigurable optical networks," Opt. Express **17**(26), 24020–24029 (2009).
8. F. Xia, L. Sekaric, and Y. A. Vlasov, "Ultra-compact optical buffers on a silicon chip," Nat. Photonics **1**(1), 65–71 (2007).
9. S. Assefa, F. Xia, W. M. J. Green, C. L. Schow, A. V. Rylyakov, and Y. A. Vlasov, "CMOS-integrated optical receivers for on-chip interconnects," IEEE J. Sel. Top. Quantum Electron. **16**(5), 1376–1392 (2010).
10. M. W. Geis, S. J. Spector, M. E. Grein, J. U. Yoon, D. M. Lennon, and T. M. Lyszczarz, "Silicon waveguide infrared photodiodes with >35 GHz bandwidth and phototransistors with 50 AW^{-1} response," Opt. Express **17**(7), 5193–5204 (2009).
11. A. H. Gnauck and P. J. Winzer, "Optical phase-shift-keyed transmission," J. Lightwave Technol. **23**(1), 115–130 (2005).
12. S. Manipatruni, Q. Xu, B. Schmidt, J. Shakya, and M. Lipson, "High speed carrier injection 18 Gb/s silicon micro-ring electro-optic modulator," *Proc. LEOS Annual Meeting* (IEEE, 2007), paper WO2.
13. A. Biberman, S. Manipatruni, N. Ophir, L. Chen, M. Lipson, and K. Bergman, "First demonstration of long-haul transmission using silicon microring modulators," Opt. Express **18**(15), 15544–15552 (2010).
14. L. Zhang, J.-Y. Yang, M. Song, Y. Li, B. Zhang, R. G. Beausoleil, and A. E. Willner, "Microring-based modulation and demodulation of DPSK signal," Opt. Express **15**(18), 11564–11569 (2007).
15. K. Padmaraju, N. Ophir, S. Manipatruni, C. B. Poitras, M. Lipson, and K. Bergman, "DPSK modulation using a microring modulator," *Proc. Conference on Lasers and Electro-Optics* (Optical Society of America, 2011), paper CTuN4.
16. A. Yariv, "Universal relations for coupling of optical power between microresonators and dielectric waveguides," Electron. Lett. **36**(4), 321–322 (2000).
17. L. Zhang, Y. Li, M. Song, R. G. Beausoleil, and A. E. Willner, "Data quality dependencies in microring-based DPSK transmitter and receiver," Opt. Express **16**(8), 5739–5745 (2008).
18. K. Padmaraju, N. Ophir, Q. Xu, B. Schmidt, J. Shakya, S. Manipatruni, M. Lipson, and K. Bergman, "Error-free transmission of DPSK at 5 Gb/s using a silicon microring modulator." *Proc. European Conference on Optical Communications* (Optical Society of America, 2011), paper Th.12.LeSaleve.2.

#162655 - $15.00 USD Received 7 Feb 2012; revised 22 Mar 2012; accepted 24 Mar 2012; published 29 Mar 2012

19. Q. Xu, S. Manipatruni, B. Schmidt, J. Shakya, and M. Lipson, "12.5 Gbit/s carrier-injection-based silicon micro-ring silicon modulators," Opt. Express **15**(2), 430–436 (2007).
20. W. Atia and R. S. Bondurant, "Demonstration of return-to-zero signaling in both OOK and DPSK formats to improve receiver sensitivity in an optically preamplified receiver," *Proc. LEOS Annual Meeting* (IEEE, 1999), paper TuM3.
21. S. Manipatruni, K. Preston, L. Chen, and M. Lipson, "Ultra-low voltage, ultra-small mode volume silicon microring modulator," Opt. Express **18**(17), 18235–18242 (2010).
22. Q. Xu, B. Schmidt, J. Shakya, and M. Lipson, "Cascaded silicon micro-ring modulators for WDM optical interconnection," Opt. Express **14**(20), 9431–9435 (2006).
23. K. Iwatsuki and J.-I. Kani, "Application and technical issues of wavelength-division multiplexing passive optical networks with colorless optical network units," J. Opt. Netw. **1**(4), C17–C24 (2009).
24. P. Dong, C. Xie, L. Chen, N. K. Fontaine, and Y.- Chen, "Experimental demonstration of microring quadrature phase-shift keying modulators," Opt. Lett. **37**(7), 1178–1180 (2012).
25. M. R. Watts, D. C. Trotter, R. W. Young, and A. L. Lentine, "Ultralow power silicon microdisk modulators and switches." *Proc. 5th IEEE International Conference on Group IV Photonics* (IEEE, 2008), pp. 4–6.
26. K. Preston, S. Manipatruni, A. Gondarenko, C. B. Poitras, and M. Lipson, "Deposited silicon high-speed integrated electro-optic modulator," Opt. Express **17**(7), 5118–5124 (2009).
27. L. Liu, J. Van Campenhout, G. Roelkens, R. A. Soref, D. Van Thourhout, P. Rojo-Romeo, P. Regreny, C. Seassal, J. M. Fédéli, and R. Baets, "Carrier-injection-based electro-optic modulator on silicon-on-insulator with a heterogeneously integrated III-V microdisk cavity," Opt. Lett. **33**(21), 2518–2520 (2008).
28. A. Guarino, G. Poberaj, D. Rezzonico, R. Degl'Innocenti, and P. Günter, "Electro–optically tunable microring resonators in lithium niobate," Nat. Photonics **1**(7), 407–410 (2007).
29. P. Rabiei, W. H. Steier, Cheng Zhang, and L. R. Dalton, "Polymer micro-ring filters and modulators," J. Lightwave Technol. **20**(11), 1968–1975 (2002).

1. Introduction

As optical communications continues to penetrate deeper into the infrastructure of information technology the need for smaller, cheaper, and more energy efficient optical components has become imperative. The last decade has seen the continued growth of fiber access networks, and the subsequent migration of fiber optic components closer to the end user [1]. Such fiber access networks, often implemented as passive optical networks (PON), typically consist of links less than 100 km, and bit rates less than or equal to 10 Gb/s [2]. While the performance metrics of these long-reach optical links are comparatively much smaller than their long-haul counterparts, the much larger breadth of access networks requires many more links, resulting in an overall increased number of optical components. At this long-reach scale, the focus on optical components shifts from performance to cost. The developing field of silicon photonics offers a revolutionary new platform for low-cost high-performance optics. Extensive research has demonstrated many of the fundamental functions needed in an optical network, such as filtering [3], modulation [4,5], switching [6,7], buffers [8], and detection [9,10], with performance characteristics comparable to their counterparts in conventional optical platforms. The complementary metal-oxide-semiconductor (CMOS)-compatible fabrication of these structures has opened up not only the possibility of low-cost, large-scale photonic integration, but also the integration of auxiliary electronics, enabling the vision of low cost transmitters and receivers for long-reach applications.

In this work, we consider the silicon microring modulator, a promising candidate for the future silicon photonic platform due to its small size, fast speed, and low energy consumption. Previous research has focused on using the microring modulator for the generation of on-off-keyed (OOK) data. In contrast, we demonstrate the first error-free generation and propagation of binary-phase-shift-keyed (BPSK) data for long-reach applications using a silicon microring modulator. The BPSK modulation format has several beneficial characteristics over OOK: a sensitivity improvement, lower susceptibility to fiber non-linearities, and reduced crosstalk in WDM systems [11]. With this demonstration we are effectively combining the benefits of silicon microring modulators and the BPSK format.

Furthermore, we compare the performance of this prototype modulator against a commercial $LiNbO_3$ phase modulator (PM), and a commercial $LiNbO_3$ Mach-Zehnder modulator (MZM), the two types of modulators most commonly used to generate BPSK data. Bit-error-rate (BER) measurements and eye patterns are used to study the evolution of transmitted microring-generated BPSK and verify its potential for use in long-reach applications.

#162655 - $15.00 USD Received 7 Feb 2012; revised 22 Mar 2012; accepted 24 Mar 2012; published 29 Mar 2012

2. Microring-modulated BPSK

The silicon microring modulator used in this work was fabricated at the Cornell Nanofabrication Facility (CNF). As depicted in Fig. 1(a), it consists of a 5-μm-radius microring side-coupled to waveguide. The microring and waveguide are designed for quasi-TE operation using a width and height of 450 nm and 200 nm, respectively. A 50-nm Si slab surrounding the microring was doped accordingly to produce a PIN structure capable of injecting carriers into the microring (Fig. 1(a)).

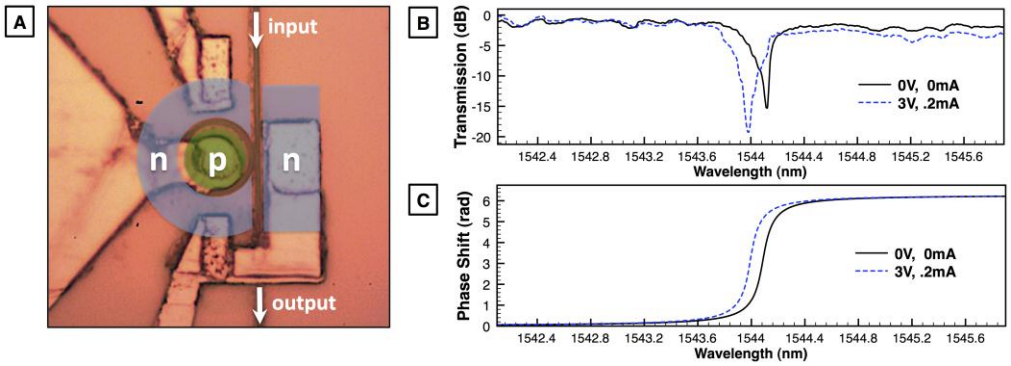

Fig. 1. (a) Microscope image of the microring modulator (doping regions are highlighted in green for p-doping and blue for n-doping) and its corresponding (b) amplitude and (c) phase response under DC conditions.

The optical resonance of the microring in its passive state is shown in Fig. 1(b). Carrier injection, enabled through the PIN structure, produces a blue shift in the resonance via the free carrier dispersion mechanism [5]. Microring modulators utilizing this device structure have been demonstrated at speeds up to 18 Gb/s [12]. Furthermore, the suitability of microring-modulated OOK for long-haul transmission has previously been verified [13].

In addition to generating traditional OOK data, it has been theorized [14] and demonstrated experimentally (at 250 Mb/s) [15] that the microring modulator is also capable of producing BPSK data. BPSK generation is enabled through the utilization of the microring's strong localized phase response. The phase response of the microring modulator can be calculated from the optical length of the microring, L, the loss in the cavity, α, and the coupling coefficient, κ [16]. Using these parameters, the field response of the microring is given by Eq. (1).

$$\frac{E_{OUT}}{E_{IN}} = \frac{-\alpha + (1-\kappa)e^{\left(\frac{-j2\pi L}{\lambda}\right)}}{-\alpha(1-\kappa) + e^{\left(\frac{-j2\pi L}{\lambda}\right)}} \tag{1}$$

Only over-coupled microrings, where $\kappa > \alpha$, exhibit the strong phase response necessary for phase modulation. This condition can be met by appropriately specifying the gap between the microring and waveguide. We use the amplitude response (Fig. 1(b)) and Eq. (1) to fit the phase response of the over-coupled microring used in this experiment. As can be seen in Fig. 1(c), the phase response of the microring blue shifts in tandem with the blue shift of the resonance. While Fig. 1(c) is a derived fit, the wavelength shift of the phase response has been confirmed through a direct measurement [15].

#162655 - $15.00 USD Received 7 Feb 2012; revised 22 Mar 2012; accepted 24 Mar 2012; published 29 Mar 2012

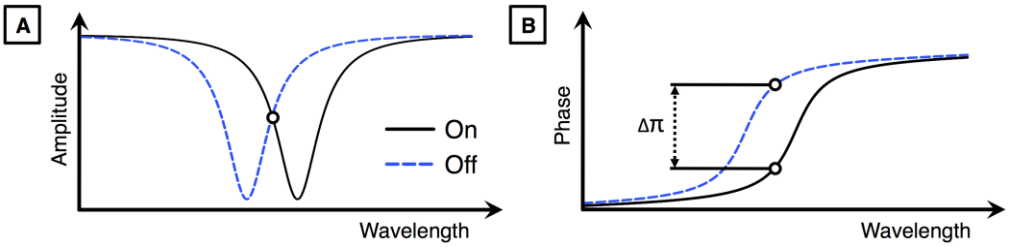

Fig. 2. BPSK generation using a microring modulator. (a) The two bit-states have equivalent amplitudes, but (b) a difference in phase of π.

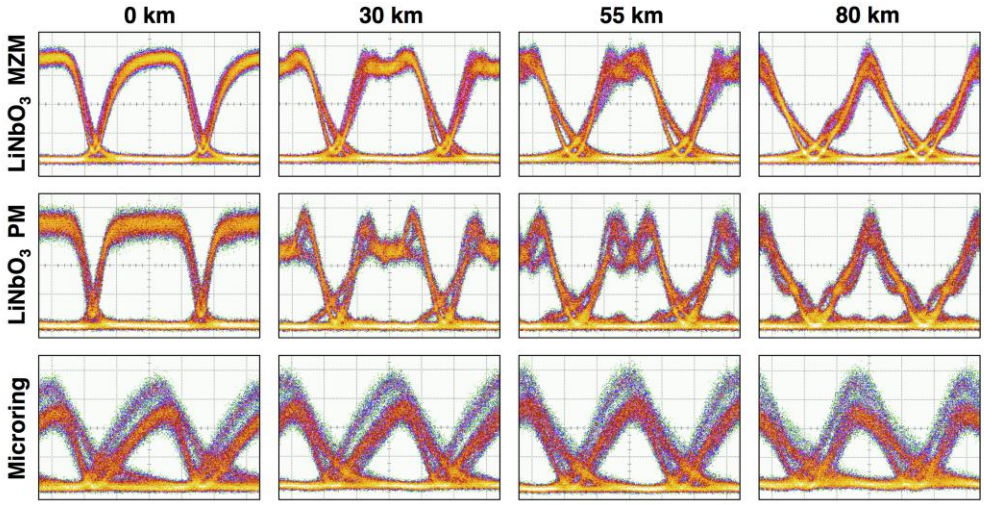

Fig. 3. Eye patterns of the demodulated BPSK signal from the $LiNbO_3$ MZM (top row), $LiNbO_3$ PM (middle row), and silicon microring modulator (bottom row) after propagating [0, 30, 55, 80] km and passing through the fiber DLI.

Similar to the generation of OOK, generation of BPSK using a microring modulator exploits a resonance shift to produce the desired bit-state. However, BPSK generation requires positioning the wavelength such that the optical bits have equivalent amplitude (Fig. 2(a)), but differ by a phase shift of π (Fig. 2(b)) [14]. A consequence of operating inside the resonance region is an inherent insertion loss completely separate from the waveguide or coupling losses. This insertion loss was approximately 3 dB for the microring modulator used in the experiment. It should be noted that while Fig. 2 depicts perfect symmetry between the two resonance states, in the carrier-injected state, free carrier absorption increases the loss in the cavity, leading the resonance to approach critical coupling. This is visible in the two resonance states depicted in the experimental measurement of Fig. 1(b), with the carrier-injected state closer to critical coupling. The asymmetry produces a pattern dependency in the demodulated BPSK signal, as seen in the experimentally demodulated BPSK signals of Fig. 3.

#162655 - $15.00 USD Received 7 Feb 2012; revised 22 Mar 2012; accepted 24 Mar 2012; published 29 Mar 2012

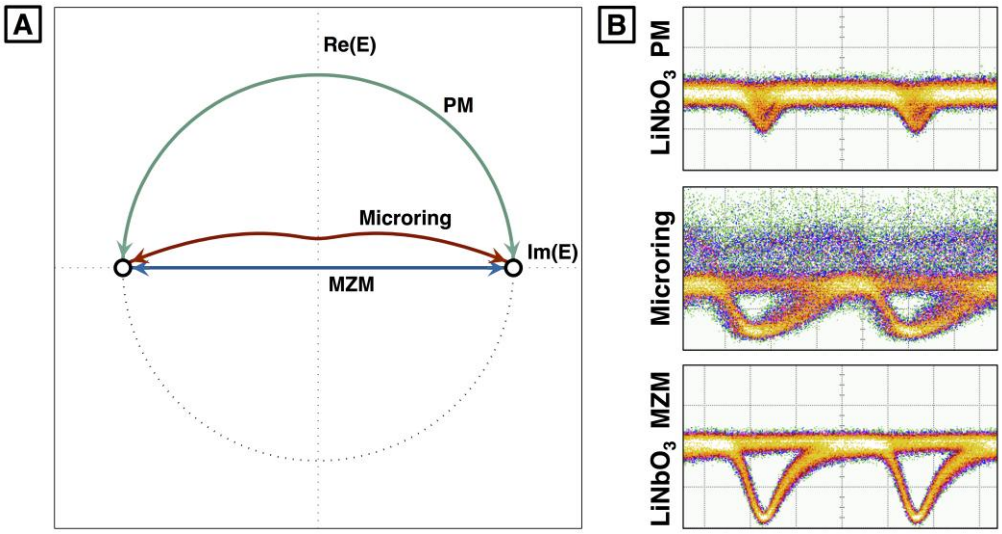

Fig. 4. (a) Signal constellation for PM-, microring-, and MZM-modulated BPSK. (b) PM-, microring-, and MZM-modulated BPSK before demodulation.

In Fig. 4, the fitted resonances of Fig. 1(b) are used to generate the signal constellation of the microring-modulated BPSK generated in this experiment. As Fig. 4 illustrates, the combination of the phase shift and amplitude dip produces a modulation mechanism unique to the microring modulator, differing from the phase modulation mechanism in either the PM or MZM [17]. The experimentally measured BPSK signals confirm that the microring modulator generates amplitude dips larger than the PM, but not reaching full extinction such as the MZM (Fig. 4(b)). It should be noted that the noise present on the microring-modulated BPSK signal of Fig. 4(b) is a result of the previously mentioned pattern dependency of the microring modulator.

The simultaneous combination of amplitude and phase modulation generates chirp characteristics that differ from those produced by the $LiNbO_3$ PM or MZM. Subsequently, it is expected that the subjection of microring-modulated BPSK to the dispersive effects of optical fiber will yield different results when compared to using BPSK generated from a PM or MZM; hence, motivating experimental measurements to validate the use of microring-modulated BPSK for long-reach applications [18].

3. Experimental setup

Our characterization consisted of generating BPSK using the aforementioned silicon microring modulator, and then propagating it through progressively longer spans of fiber while observing the deformation of the eye pattern and changes in the bit-error-rate. In the experimental setup, (Fig. 5), a pulsed-pattern generator (PPG) was used to generate a 5-Gb/s non-return-to-zero (NRZ) 2^7-1 pseudo-random bit sequence (PRBS) electrical signal. The 1-V_{pp} signal was biased at 1.2 V and conditioned with a pre-emphasis circuit to enable high-speed operation of the modulator [19]. A CW tunable laser at a wavelength of 1544 nm was set to a TE polarization before being launched onto the chip. The microring-modulated BPSK signal egressing from the chip was amplified with an erbium-doped fiber amplifier (EDFA), and filtered (λ), before being passed into [0, 30, 55, 80] km of single-mode fiber (SMF) at a power of 11 dBm. The varying lengths of fiber result in variable amounts of accrued loss; hence, a variable optical attenuator (VOA) was used to attenuate the signal to a fixed power of –17 dBm, thereby ensuring OSNR consistency between measurements. This signal was then amplified and filtered before being passed into a thermally stabilized delay line interferometer (DLI) to demodulate the BPSK signal. Because the differential of PRBS is equivalent to the original PRBS, error testing is possible without the customary differential-phase-shift-keying

#162655 - $15.00 USD Received 7 Feb 2012; revised 22 Mar 2012; accepted 24 Mar 2012; published 29 Mar 2012

(DPSK) encoder and decoder. The demodulated signal was received using a PIN-TIA photodetector followed by a limited amplifier (LA) and fed to a bit-error-rate tester (BERT) for BER measurements. In addition, a digital communications analyzer (DCA) was used to record eye patterns.

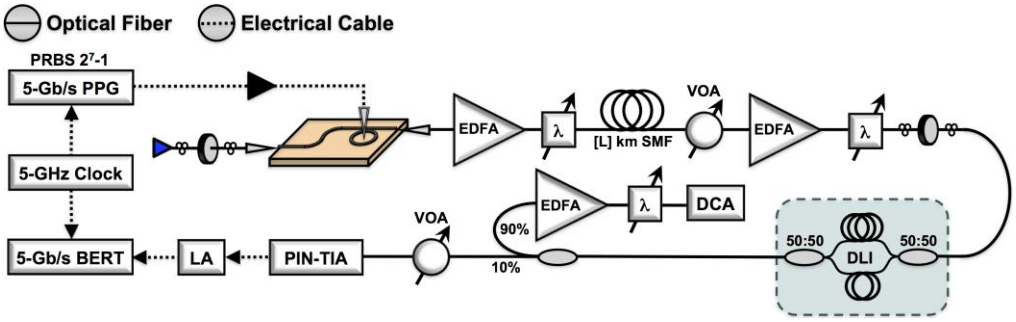

Fig. 5. Experimental setup for bit-error validation of microring-modulated BPSK.

For comparison, a commercial $LiNbO_3$ dual-drive MZM (rated for 10-Gb/s operation) was inserted in place of the microring modulator. In this setup, both the inverted and non-inverted ports of the PPG are used to generate 4-V_{pp} electrical signals that drive the MZM in a push-pull configuration, producing the desired BPSK. The launch and exit powers of the fiber span were also maintained at 11 dBm and −17 dBm, respectively, to ensure consistency with the characterization of the microring-modulated BPSK. Similarly, a commercial $LiNbO_3$ single-arm PM (also rated for 10-Gb/s operation) was characterized in the same configuration, using a single output of the PPG to generate the 6-V_{pp} electrical signal needed to drive the PM.

4. Experimental results

Figure 3 depicts the eye patterns for the constructive port of the demodulated BPSK signals as they propagate through the progressively increasing fiber spans. For the PM- and MZM-modulated BPSK signals, the chirp induced from the modulation results in a gradual NRZ to RZ conversion of the demodulated signal. A similar phenomenon occurs with the microring-modulated BPSK signal. However, from the eye diagrams, it is observed that the fiber span at which the microring-modulated BPSK signal reaches an optimal RZ format occurs sooner (at 55 km) when compared to the PM- or MZM-modulated BPSK signal.

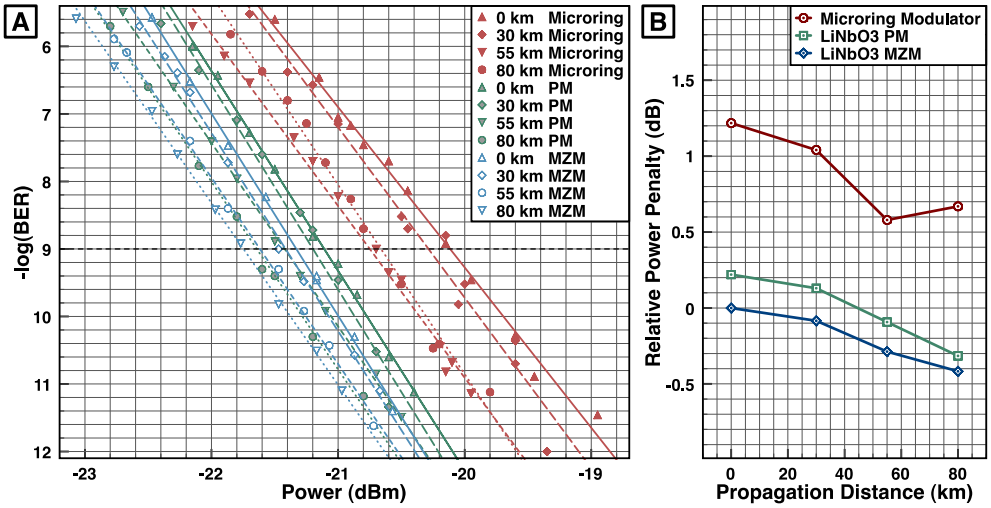

Fig. 6. (a) BER curves. (b) Power penalties taken relative to 0-km propagation of the $LiNbO_3$ MZM-modulated BPSK signal.

#162655 - $15.00 USD Received 7 Feb 2012; revised 22 Mar 2012; accepted 24 Mar 2012; published 29 Mar 2012

This behavior is further validated by the BER measurements (Fig. 6(a)) conducted on the corresponding demodulated BPSK signals of Fig. 3. Error-free performance, defined as a 10^{-12} error-rate, is confirmed for microring-modulated BPSK up to the maximally tested fiber span of 80 km. The power-penalties, as measured at the 10^{-9} error-rate point, and referenced to the 0-km propagation of the MZM-modulated BPSK, are summarized in Fig. 6(b). The chirp-induced NRZ to RZ conversion results in better receiver sensitivity, and hence negative power-penalty relative to the power-penalty with no fiber propagation [20]. The fiber-propagated behavior of the PM- and MZM-modulated BPSK are similar, exhibiting gradually decreasing power-penalties until finally reaching power penalties of −0.5 dB and −0.4 dB, respectively, relative to their 0-km propagation. As expected and indicated by the measurements, the PM-modulated BPSK signal suffers from more chirp than the MZM-modulated BPSK signal.

In contrast, the microring-modulated BPSK, as was noted from the eye patterns, achieves its lowest power-penalty at 55 km. More importantly, the power-penalty of the microring modulator relative to the MZM is less than 1.3 dB throughout the 80-km propagation of the signal. Because the bandwidth of the microring modulator is lower than that of the MZM or PM, a direct comparison of the chirp-induced propagation is not possible. Regardless, this demonstration shows that the relative power-penalty variance of the microring-modulated BPSK is on par with the commercial MZM and PM.

5. Discussion and conclusion

We have demonstrated error-free generation of BPSK using a microring modulator at a commercially viable data rate of 5 Gb/s. Furthermore, it was shown that this signal can be propagated up to 80 km with a small (< 1dB) variance in its power penalty, illustrating its resilience to chromatic dispersion and validating its use in the aforementioned long-reach applications. As the bit-error-rate measurements showed, this prototype silicon microring modulator has performance comparable to the commercial modulators normally used for the generation of BPSK. In addition, the silicon microring modulator has several advantages that would render it preferable over the traditional $LiNbO_3$ PM or MZM.

One advantage of note is the considerably lower drive voltage used for the microring modulator, 1-V_{pp}, versus the 4-V_{pp} and 8-V_{pp} required for the $LiNbO_3$ PM and MZM, respectively. The required drive voltage can be further decreased to sub-volt levels by scaling down the size of the microring modulator, simultaneously reducing the footprint of the device [21]. The low-voltage operation of the microring modulator can enable high-speed optical links while expending with the expensive, high-speed electronic amplifiers normally required. In addition, the wavelength selectivity of the microring modulator can be exploited, enabling the cascading of microring modulators for high-bandwidth wavelength-division-multiplexed (WDM) operation [22]. These advantages are magnified when considering the economy of scale found in long-reach applications, where the low-voltage, integrated WDM operation of microring modulators can translate to a drastic reduction in the number of individual components. As long-reach networks continue to migrate to from PON to WDM-PON, the need for low-cost, integrated photonics, will only further justify the use of microring modulators [23]. Furthermore, recent demonstrations have shown that a combination of microring-modulated BPSK can produce microring-modulated QPSK signals, foreshadowing its potential use in future long-haul communication networks where QPSK is the preferred next-generation modulation format [24].

Lastly, we conclude by noting the generalizability of these results. While, in this instance we utilized a silicon microring modulator for the aforementioned advantages, any resonator based device that obeys Eq. (1) will display similar behavior. Current realizations of these types of modulators include devices also in the silicon-on-insulator platform, such as microdisk modulators, or devices implemented in other material platforms, such as poly-silicon, III-Vs, $LiNbO_3$, or polymers [25–29].

#162655 - $15.00 USD Received 7 Feb 2012; revised 22 Mar 2012; accepted 24 Mar 2012; published 29 Mar 2012

Acknowledgments

This work was supported in part by the NSF through CIAN ERC under Grant EEC-0812072, and in part by the NSF and Semiconductor Research Corporation under Grant ECCS-0903406 SRC Task 2001.

#162655 - $15.00 USD Received 7 Feb 2012; revised 22 Mar 2012; accepted 24 Mar 2012; published 29 Mar 2012